Sb-rich rutile in the manganese concentrations at St. Marcel-Praborna, Aosta Valley, Italy: petrology and crystal-chemistry

DAVID C. SMITH[1] AND ELENA-ADRIANA PERSEIL[1,2]

[1] Laboratoire de Minéralogie, Muséum National d'Histoire Naturelle, 61 Rue Buffon, 75005 Paris, France
[2] CNRS, Unité de Recherche Associée n° 736, 61 Rue Buffon, 75005 Paris, France

Abstract

The petrographical, crystal-chemical and petrogenetical aspects of rutile rich in antimony (up to 33.75 wt.% Sb_2O_5; equal to 0.2 Sb^{5+} per O = 2) from St. Marcel-Praborna in the Aosta Valley, Italy, were re-examined. These compositions occur in two different petrographical environments (within the rock matrix or as microinclusions within Sb-rich titanite) in the manganese concentrations at this locality. The new data confirm our earlier hypothesis that two distinct petrogenetical/crystal-chemical processes both occurred: 1. Sb-metasomatism of pre-existing Sb-free rutile inclusions; and 2. creation of neoblastic Sb-rich rutile by the expulsion of Ti from pre-existing Sb-free titanite being metasomatized by Sb to form Sb-rich titanite. In the literature, Sb in minerals is variably considered as being trivalent and/or pentavalent. This work demonstrates that within rutile it is entirely Sb^{5+}, substituting for Ti^{4+} by the following heterovalent cation exchange mechanism which is also the dominant one in the host Sb-rich titanite: $2\ ^{vi}R^{4+} = {}^{vi}R^{3+} + {}^{vi}R^{5+}$, where $^{vi}R^{3+} = (Al,Cr,Mn,Fe)^{3+}$. A near-perfect correlation of ΣR^{5+} *vs.* ΣR^{3+} ($r > 0.98$) is perturbed only by the presence of trace amounts of Ca^{2+}, Sr^{2+} and Ba^{2+}. Traces of Mn^{4+}, Si^{4+} and/or $(OH)^-$ might also be present. These alkaline earth cations are the largest cations ever recorded in the rutile structure and are seemingly too large to occupy normal octahedral sites. The cation exchange mechanism involved might be that found in the 'trirutile' mineral group: $3\ ^{vi}R^{4+} = {}^{vi}R^{2+} + 2\ ^{vi}R^{5+}$. Alternatively these large divalent cations may be situated in the lozenge-shaped tunnels of the rutile structure, by analogy with other large cations occupying the wider subrectangular tunnels in the analogous cryptomelane/hollandite/priderite, romanéchite and todorokite mineral groups. This leads to a possible new cation exchange mechanism for the rutile structure: $2\ ^{vi}R^{4+} + {}^{tunnel}vacant = 2\ ^{vi}R^{3+} + {}^{tunnel}R^{2+}$.

KEYWORDS: antimony, rutile, titanite, roméite, crystal-chemistry, petrology, St. Marcel-Praborna, Italy.

Introduction

THIS article examines in detail the crystal-chemistry, and briefly the petrology, of the Sb-rich rutile in our samples from the celebrated manganese concentrations at St. Marcel-Praborna, Val d'Aosta, Italy. A substantial bibliography concerning the complex mineralogy at this locality has been provided in Perseil and Smith (1995) who described in detail the Sb-rich titanite occurring there. Rutile has a very wide *P-T* (pressure-temperature) stability field at all *T* at $P < \sim 50$ kbar since the polymorphs anatase and brookite are considered as metastable phases (Lindsley, 1991). However rutile is most commonly created during metamorphism at medium to high *T*. Rutile in sedimentary rocks is generally considered as being of detrital origin. Thus the growth of rutile at relatively low *T*, like during the late stages of retrograde metamorphism at St. Marcel-Praborna, seems to be rather unusual.

The presence of Sb in the rutile structure has been mentioned by several authors (e.g. Heslop and Robinson, 1963; Parent and Roger, 1968; Roger, 1972; Graham and Morris, 1973; Foord *et al.*, 1991; Perseil, 1991; Perseil and Smith, 1995). In addition to the first petrographical environment of Sb-rich rutile (late-stage veinlets II, see below) recorded at St. Marcel-Praborna by Perseil (1991), a second petrographical environment (dislocated late-stage veinlets III, see below) was mentioned by Perseil and Smith

Mineralogical Magazine, October 1997, Vol. 61, pp. 655–669

(1995) and Smith and Perseil (1996). Both environments are re-examined here and new petrographical data are presented.

Concerning the crystal-chemistry, the same problem over the valency of Sb (and also of Cr, Mn and Fe) exists in rutile as in titanite (Perseil and Smith, 1995) and roméite (Perseil and Smith, in prep.), i.e. Sb^{3+} as in senarmontite and valentinite (both = $Sb_2^{3+}O_3$), or Sb^{5+} as in swedenborgite ($NaBe_4Sb^{5+}O_7$), or both Sb^{3+} and Sb^{5+} as in cervantite $Sb^{3+}Sb^{5+}O_4$ or stibiconite $Sb^{3+}Sb_2^{5+}O_6(OH)$ (Fleischer and Mandarino, 1995). The general cation exchange:

$$2\ {}^{vi}R^{4+} = {}^{vi}R^{3+} + {}^{vi}R^{5+} \quad (1)$$

and more specifically the mechanism:

$$2\ {}^{vi}Ti^{4+} = {}^{vi}[Al^{3+} + Cr^{3+} + Mn^{3+} + Fe^{3+}] + {}^{vi}Sb^{5+} \quad (2)$$

is shown here to be predominant in the Sb-rich rutiles of St. Marcel-Praborna (both environments II and III), as is the case in the host Sb-rich titanites (Perseil and Smith, 1995) and in various other Ti-Mn-Fe oxides or silicates (Moore, 1968, [who did not include Al and Cr]). An end-member at the Ti-free extreme of this substitution is known since the compound $FeSbO_4$ has the rutile structure (Heslop and Robinson, 1963, p. 350). This is the ideal composition of the mineral squawcreekite (Foord *et al.*, 1991) found in the Black Range tin district of New Mexico, but the natural samples contain considerable replacement of Ti^{4+} by Sn^{4+}.

This paper also addresses the interesting crystal-chemical problems raised by the possible presence of Mn^{4+}, Si^{4+} and/or $(OH)^-$ in Sb-rich rutile, and by the uncertain crystallographic location of the large divalent cations Ca^{2+}, Sr^{2+} and Ba^{2+} detected therein; a new model is presented concerning this latter point.

Geological/geochemical context

The geological context of the manganese concentrations at St. Marcel-Praborna was briefly summarized recently by Perseil and Smith (1995) on the basis of various publications, notably Perseil (1985), Mottana (1986) and Martin and Kienast (1987). Here it is just recapitulated that these concentrations, in which many Mn-rich or Mn-poor mineral species occur, are restricted to a 4 to 8 m thick quartzite unit of diverse parageneses, textures and colours. This unit represents the heterogeneous basal part of the sedimentary cover of an ophiolite suite. All these units together constitute a part of the Piemont Nappe which was metamorphosed up to the eclogite facies (jadeite present) in Cretaceous times and was retrogressed in the early Tertiary through several post-eclogite stages terminating in the greenschist facies. These manganese concentrations were subsequently penetrated by several networks of cross-cutting veins and late fractures which were responsible for the mobility of certain elements, in particular H, Na, K, Ca, Sr, Ba, Cr, Fe and Sb, most of which came from outside as metasomatic influxes. Arsenic is now added to this list, as it enters both titanite and apatite (Perseil and Smith, 1996; Perseil *et al.*, 1996).

Petrographical/petrogenetical data

Three distinct petrographical environments of Sb-rich titanite were recognized by Perseil and Smith (1995):

I. The Emerald-Green Horizon: a green pyroxene-bearing feldspathic quartzite.

II. Late-stage cm-sized veinlets cutting an amphibole-rich dark-grey-green amphibolite.

III. Microfissured late-stage mm-sized veinlets cutting an albite-rich magnetite-rich light-grey-green amphibolite.

Sb-free rutile occurs in the matrix of environment I, but Sb-rich rutile occurs in the matrices of environments II (especially in the proximity of Sr-bearing piemontite: Perseil, 1991; and new data in Figs. 1–4 here) and III. Sb-rich titanite contains microinclusions of Sb-free rutile in environments I and II, but of Sb-rich rutile in environment III where it is often accompanied by the rare Sb-rich mineral roméite (Perseil and Smith, 1995; Smith and Perseil, 1996; and new data in Figs. 5–6 here).

Several petrogenetical questions concerning Sb-rich titanite posed and discussed by Perseil and Smith (1995) are relevant to the Sb-rich rutile. Whereas the

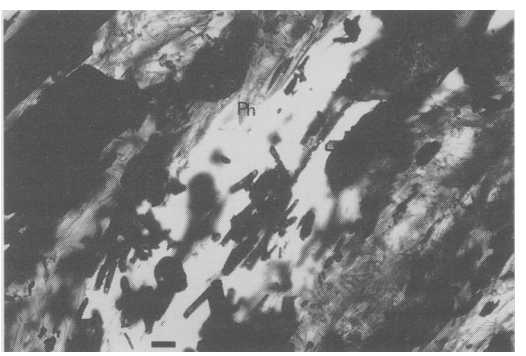

FIG. 1. Environment II. Plane polarized light. Scale bar = 40 μm. Elongated crystals of Sb-rich rutile occurring within the quartz-rich matrix but close to grains of piemontite (dark) associated with Mn-bearing phengite (Ph).

growth of the titanites in the veinlets (environments II and III) was obviously a syn-veinlet event, it was not obvious if: (a) late Sb had replaced Ti in pre-existing Sb-free titanite grains (metasomatism), or if (b) the Sb-rich titanite zones represented later overgrowths (neoblasts). Evidence for each process was recorded. It was also suggested that two essentially comparable processes of 'antimonization' of titanite and of rutile were contemporaneous, i.e. the two processes possible in titanite were both possible in rutile: metasomatism = process (c); neoblasts = process (d). However, given process (a), what had happened to the Ti atoms in the titanite displaced by the Sb (and the accompanying R^{3+}) atoms? Three processes were suggested, each one being supported by some evidence:(e) minimal migration of Ti with the creation *in situ* of neoblasts of Sb-rich rutile microinclusions, i.e. process (d) and thus not process (c); (f) migration of Ti to the borders of the titanite crystals where it became fixed in a narrow overgrowth zone of neoblastic Sb-rich titanite, i.e. process (b); or (g) maximal migration of Ti further into the matrix to be fixed in Ti-rich braunite and Ti-rich hollandites.

It is perhaps important to emphasize that Sb-free rutile commonly occurs elsewhere in these rocks in environments not concerning Sb-rich titanite, such as inclusions within other phases, especially garnet, clinopyroxene or clinoamphibole. Presumably these phases acted as barriers impermeable to the penetration of Sb^{5+}, although they were not impermeable to such cations as Al^{3+}, Cr^{3+}, Mn^{3+}, Fe^{3+} or Ti^{4+} which can enter these crystal structures much more easily than any pentavalent cation. Alternatively the Sb-metasomatism was spatially limited to the immediate proximity of the veinlets of environments II and III and their respective networks of microfractures.

Figures 2,3,4 and 6 provide critical new data. The zoning in mean atomic number Z detectable with back-scattered SEM images of rutile (Fig. 4) is clearly oscillatory in nature. This texture is generally attributed to variations in the composition of migrating fluids (e.g. Morgan, 1975; Yardley *et al.*, 1991; Lasnier *et al.*, 1992). Significant oscillatory zoning was not observed by Perseil and Smith (1995) in the Sb-rich titanites but extensive infiltration metasomatism by Sb was nevertheless deduced; some new unpublished data reveals oscillatory zoning in the titanites, especially near grain boundaries. In their review, Yardley *et al.* (1991) argued that oscillatory zoning in metamorphic rocks is promoted by the introduction of a fluid not in equilibrium with the pre-existing mineral assemblage and they suggest that this texture can be used to characterise infiltration metasomatism. On this basis the oscillatory zoning in the Sb-rich titanites and Sb-rich rutiles strongly supports our previously-suggested processes (a) and (c) respectively.

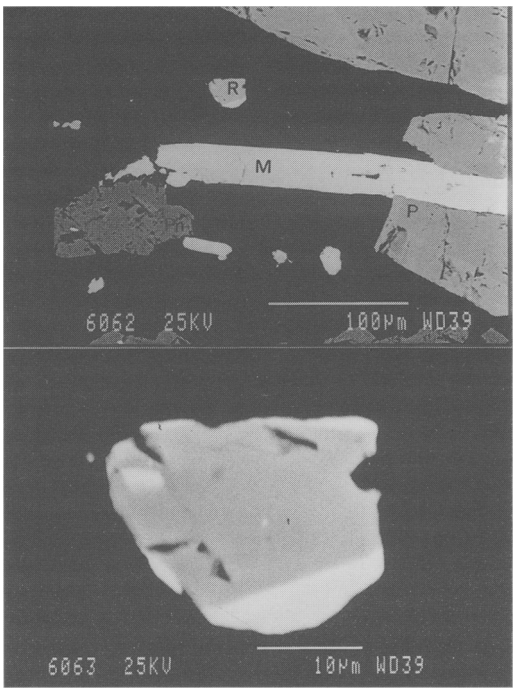

FIG. 2. Environment II. Back-scattered SEM image with enlargement below. An equant Sb-rich rutile crystal (R) near to elongate magnetite (M), prismatic piemontite (P) and lath-like Mn-bearing phengite (in the matrix) occurring at the edge of an albitic veinlet.

However the complex zoning revealed in Fig. 4 permits the possible recognition of both processes (c) and (d) in the same grain of rutile. The central dark core is inferred to be an original feature of the first crystallization of Sb-free rutile in the veinlet mineral assemblage. The first white oscillatory zoned band is attributed to Sb infiltration metasomatism by process (c). The relatively large medium-grey parts on either side of the core are still quite rich in Ti and are attributed to neoblastic growth of rutile by process (d) caused by the arrival of extra Ti expelled from Sb-metasomatized titanite by process (a). The final outer white oscillatory zoned band is attributed to a second stage of Sb infiltration metasomatism, but presumably belonging to the same geological event. Note that the first white band actually reaches the grain boundary; this could alternatively mean that both white bands were contemporaneous and that Sb penetrated later between core and neoblastic rutile.

Where the Sb-rich rutile grains are less than about 10 µm in size, oscillatory zoning is not observed. The

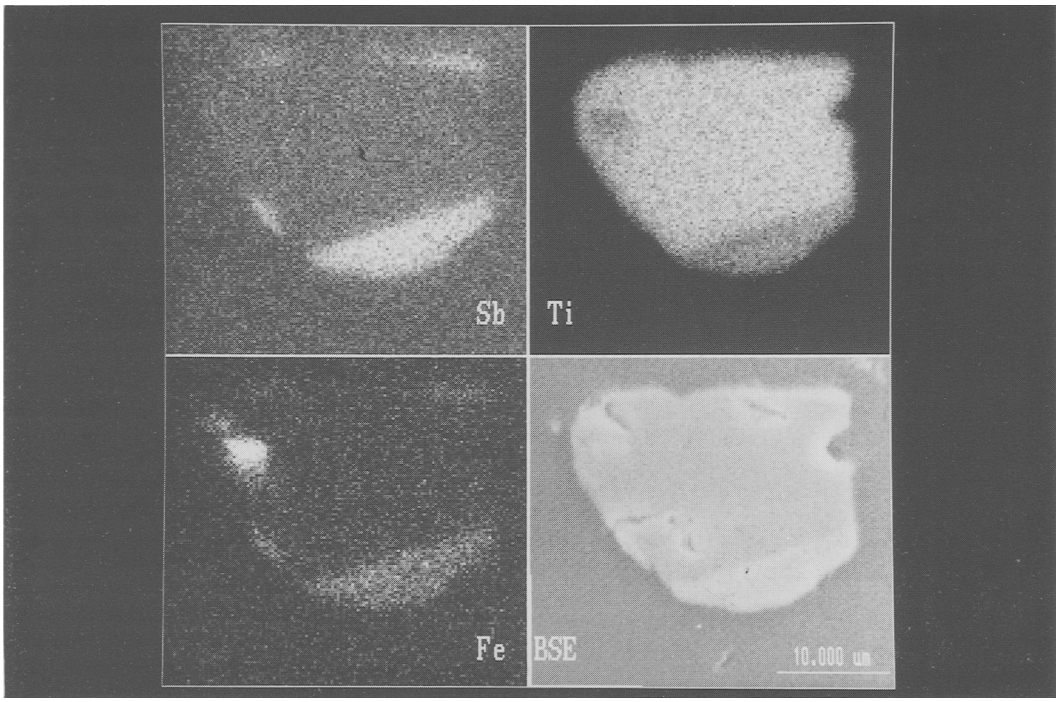

FIG. 3. Environment II. Back-scattered and X-ray SEM images of the isolated rutile of Fig. 2. Note the top and bottom zones rich in Sb and Fe but poor in Ti. The Fe-rich, Sb-poor and Ti-poor patch at the left is magnetite.

detailed SEM X-ray images (Figs. 3, 6) clearly show that Fe, and to a lesser extent Mn, follow Sb in their antipathy to Ti. The textures of Fig. 3 favour Sb metasomatism by process (c) in the matrix of environment II. The process involved is less clear in the microinclusions of environment III (Fig. 6), but it is easier to explain the Sb presence by neoblastic growth by process (d) since there is a ready source of expelled Ti within this metasomatized titanite. In conflict with this is the observation that the Sb-Fe-rich end of this rutile microinclusion points away from the Sb-Fe-rich part of the host titanite such that the whole rutile grain could have been pre-existing and metasomatized by process (c).

Mineral chemical data

Analytical methods

The rocks were mounted in polished thin sections and were examined by transmitted and reflected light microscopy, and scanning electron microscopy (SEM) with backscattered electron images and/or X-ray elemental mapping. The minerals were analysed with the CAMEBAX electron microprobe (EMP) at the Muséum National d'Histoire Naturelle (Paris) under the operating conditions already listed in Perseil and Smith (1995) except for the addition of the standard metal Zr for Zr L_α (and, as a correction of a printing error in the 1995 paper: wollastonite for Si K_α, not L_α). Other elements were searched for by EMP (WDS and/or EDS) but were not detected in amounts exceeding 0.005 wt.%.

The EMP analyses, each of which is the mean of at least six nearly-identical point analyses, are presented in order of increasing Sb_2O_5 content in Table 1. Since the size of some rutile grains is in the order of only a few microns, a few of these analyses could be 'contaminated' by the partial addition of elements from the host phase, especially Ca, Ti or Si where titanite is the host. Since the rutile structure does not provide a tetrahedral site suitable for Si (see below for Si in the octahedral site), all analyses with Si exceeding 0.33 wt.% SiO_2 (= 0.005 Si per O = 2 in rutile) were rejected; for those analyses with 0.01–0.20 wt.% SiO_2 in rutile (2 out of 9), the analyses were maintained except that Si was excluded from calculation of the structural formulae

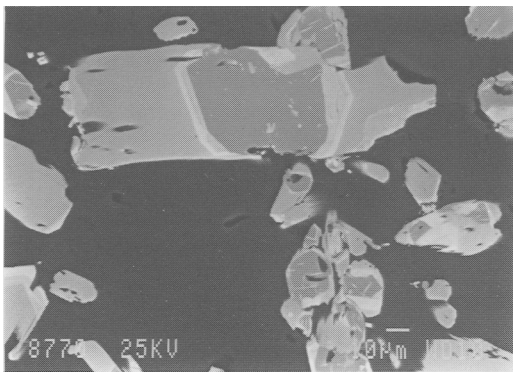

FIG. 4. Environment II. Back-scattered SEM image of several grains of Sb-rich rutile revealing extensive but complex oscillatory zoning where the lighter colour indicates greater average Z (i.e. Sb + Fe) except that the narrow parallel lamellae are of hematite. Note that the largest grain reveals successively: – a core poor in Sb (original veinlet rutile); – a first rim very rich in Sb (? Sb-metasomatism of the core); – large overgrowths on two sides which are moderately rich in Sb (neoblasts); and – a final outer rim (? Sb-metasomatism of the neoblasts).

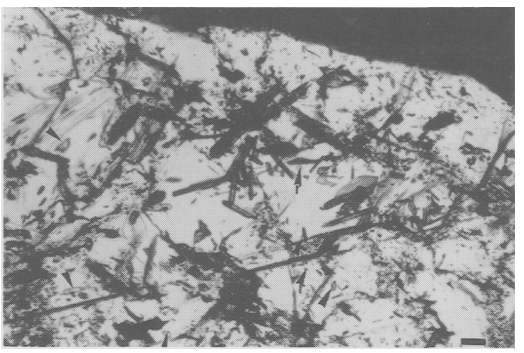

FIG. 5. Environment III. Plane polarised light. Scale bar = 50 μm. Sb-rich titanite grain full of inclusions of Sb-rich rutile (dark and elongate), magnetite (black), and small grains of roméite (r) indicated by small or large arrows according to their relative size.

on the assumption that it represents a minor contamination. This exclusion was not done on a supposed basis that this is the 'correct' approach; it is simply a working hypothesis amongst several possible calculation methods, none of which can be shown to be uniquely correct. Ca was undetected in the listed analyses, but traces were often found in other analyses not listed; for this reason Ca^{2+} is mentioned alongside the other divalent alkaline earth cations. An estimation of the analytical precision is given in Table 1 by the standard deviation (1 sigma) values derived from repetitive analyses on or very close to a single electron impact point.

Ion substitutions in the rutile structure

The rutile structure is composed of parallel chains of edge-sharing octahedra along the *c* direction; these chains are cross-linked through octahedral corners to form nearly-square lozenge-shaped tunnels which have ideally the same geometry, frequency and topology as the chains. In a hexagonal close-packed plane of oxygens this arrangement corresponds to alternating lines of occupied and vacant octahedral interstices (*e.g.* Fig. 6 in Waychunas, 1991). The resulting space group is $P4_2/mnm$, i.e. tetragonal but without a simple tetrad symmetry axis, and there is

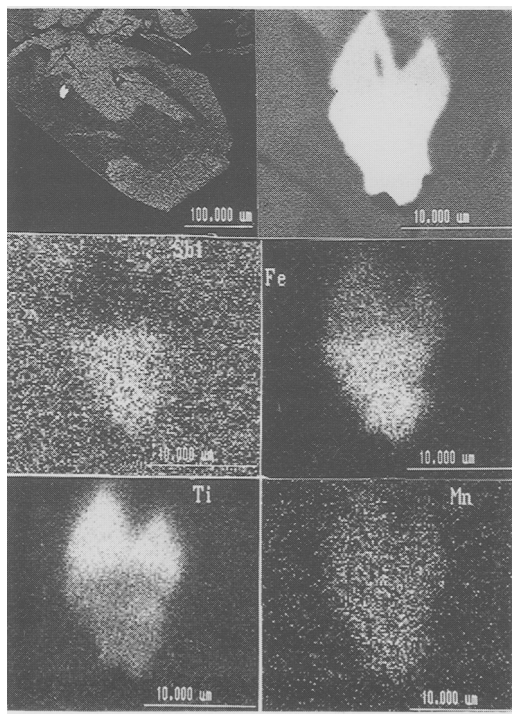

FIG. 6. Environment III. Back-scattered SEM image of a double-pointed equant Sb-rich rutile inclusion within titanite, with an enlargement and four X-ray images thereof. Note that the pointed end is Ti-rich whereas the other end is rich in Sb and Fe and less so in Mn. The printed 10.000 μm scale bar means ten, not ten thousand, μm (cf. Fig. 3).

TABLE 1. EMP analyses of Sb-rich rutile from environments II (1–5) and III (6–9)

	1	2	3	4	5	*sigma*	6	7	8	9
CaO	0.00	0.00	0.00	0.00	0.00	*0.00*	0.00	0.00	0.00	0.00
SrO	0.42	0.53	0.25	0.41	0.36	*0.20*	0.62	0.50	0.41	0.47
BaO	0.00	0.00	0.00	0.02	0.00	*0.20*	0.00	0.00	0.06	0.00
Al_2O_3	0.00	0.04	0.04	0.04	0.00	*0.04*	0.00	0.13	0.16	0.27
Cr_2O_3	0.13	0.17	0.18	0.09	0.16	*0.03*	0.09	0.00	0.07	0.04
Mn_2O_3	1.11	1.12	1.23	1.41	1.43	*0.13*	1.73	1.79	1.68	1.66
Fe_2O_3	5.28	7.84	13.41	12.39	14.19	*0.31*	12.96	13.58	14.27	15.45
SiO_2	0.00	0.00	0.00	0.06	0.00	*0.17*	0.00	0.00	0.20	0.00
TiO_2	79.62	74.21	55.09	54.67	51.53	*0.20*	52.45	51.64	51.06	48.63
ZrO_2	0.00	0.00	0.01	0.00	0.05	*0.01*	0.00	0.00	0.01	0.00
Sb_2O_5	12.23	15.84	30.00	31.44	32.78	*0.49*	30.18	31.41	32.72	33.75
Total	98.79	99.75	100.21	100.53	100.50		98.03	99.05	100.64	100.27
Structural formulae on the basis of sum (cations) = 1										
Ca^{2+}	0.000	0.000	0.000	0.000	0.000	*0.000*	0.000	0.000	0.000	0.000
Sr^{2+}	0.004	0.004	0.002	0.004	0.003	*0.002*	0.006	0.005	0.004	0.004
Ba^{2+}	0.000	0.000	0.000	0.000	0.000	*0.002*	0.000	0.000	0.000	0.000
Al^{3+}	0.000	0.001	0.001	0.001	0.000	*0.001*	0.000	0.002	0.003	0.005
Cr^{3+}	0.001	0.002	0.002	0.001	0.002	*0.001*	0.001	0.000	0.001	0.001
Mn^{3+}	0.012	0.012	0.015	0.017	0.017	*0.002*	0.021	0.022	0.020	0.020
Fe^{3+}	0.057	0.086	0.158	0.147	0.169	*0.003*	0.157	0.163	0.170	0.186
Ti^{4+}	0.860	0.810	0.648	0.647	0.615	*0.002*	0.635	0.621	0.609	0.584
Zr^{4+}	0.000	0.000	0.000	0.000	0.000	*0.000*	0.000	0.000	0.000	0.000
Sb^{5+}	0.065	0.085	0.174	0.184	0.193	*0.003*	0.180	0.187	0.193	0.200
sum (cations)	1.000	1.000	1.000	1.000	1.000		1.000	1.000	1.000	1.000
sum (oxygens)	1.994	1.988	1.997	2.005	1.999		1.995	1.995	1.995	1.990
oxygen excess	−0.006	−0.012	−0.003	0.005	−0.001		−0.005	−0.005	−0.005	−0.010
sum R^{2+}	0.004	0.004	0.002	0.004	0.003		0.006	0.005	0.004	0.004
sum R^{3+}	0.071	0.101	0.175	0.165	0.189		0.179	0.188	0.194	0.211
sum R^{4+}	0.860	0.810	0.648	0.647	0.615		0.635	0.621	0.609	0.584
sum R^{5+}	0.065	0.085	0.174	0.184	0.193		0.180	0.187	0.193	0.200
sum $R^{5+}-R^{3+}$	−0.005	−0.015	−0.001	0.018	0.004		0.001	−0.001	−0.002	−0.011
sum $R^{5+}-R^{3+}-R^{2+}$	−0.009	−0.020	−0.003	0.014	0.001		−0.005	−0.006	−0.006	−0.016
Charge total	3.988	3.976	3.994	4.011	3.998		3.990	3.990	3.990	3.980
Charge excess	−0.012	−0.024	−0.006	0.011	−0.002		−0.010	−0.010	−0.010	−0.020
* $[R^{5+}-R^{3+}]$	−0.005	−0.015	−0.001	0.018	0.004		0.001	−0.001	−0.002	−0.011
* $[R^{5+}-R^{3+}-2xR^{2+}]$	−0.012	−0.024	−0.006	0.011	−0.002		−0.010	−0.010	−0.010	−0.020

* charge difference with respect to R^{4+}

only one kind of octahedral site such that cation ordering is impossible.

Although the ideal formula for rutile is $Ti^{4+}O_2^{2-}$, various chemical impurities have often been mentioned in the literature. Ti^{4+} may be replaced by major amounts of Fe^{3+}, Nb^{5+} and/or Ta^{5+}, by minor amounts of Al^{3+}, V^{3+}, Cr^{3+}, and/or Sn^{4+}, and/or by trace amounts of Mg^{2+}, Mn^{2+}, Fe^{2+}, Ca^{2+} and/or Si^{4+} according to the reviews by El Goresy (1976*b*), Rumble (1976), Frost (1991), Haggerty (1991) and Deer *et al.* (1992, p. 548–51). Putnis (1978) and Pinet and Smith (1985) recognized hematite exsolution from rutile, and Smith (1988) suggested corundum exsolution. Lindsley (1991) compiled experimental work demonstrating limited solid-solution in rutile of Fe_2O_3 and, apparently, also of FeO.

TABLE 2. Mineral names and chemical formulae of 'ideal' natural oxide compositions having the tetragonal crystal structure of rutile $^{vi}R^{4+}\ ^{iii}O_2^{2-}$

Formula	Name	Formula per O = 12
Single cation		
$Ge^{4+}_1O_2$	argutite	$Ge^{4+}_6O_{12}$
$Mn^{4+}_1O_2$	pyrolusite	$Mn^{4+}_6O_{12}$
$Pb^{4+}_1O_2$	plattnerite	$Pb^{4+}_6O_{12}$
$Si^{4+}_1O_2$	stishovite	$Si^{4+}_6O_{12}$
$Sn^{4+}_1O_2$	cassiterite	$Sn^{4+}_6O_{12}$
$Te^{4+}_1O_2$	paratellurite	$Te^{4+}_6O_{12}$
$Ti^{4+}_1O_2$	rutile	$Ti^{4+}_6O_{12}$
Double cation disordered		
$Fe^{3+}_1Sb^{5+}_1O_4$	squawcreekite	$Fe^{3+}_3Sb^{5+}_3O_{12}$
Double cation ordered ('trirutile')		
$Fe^{2+}_1Sb^{5+}_2O_6$	tripuhyite	$Fe^{2+}_2Sb^{5+}_4O_{12}$
$Mg^{2+}_1Sb^{5+}_2O_6$	byströmite	$Mg^{2+}_2Sb^{5+}_4O_{12}$
$Zn^{2+}_1Sb^{5+}_2O_6$	ordoñezite	$Zn^{2+}_2Sb^{5+}_4O_{12}$
$Fe^{2+}_1Nb^{5+}_2O_6$	ferrotapiolite	$Fe^{2+}_2Nb^{5+}_4O_{12}$
$Mn^{2+}_1Nb^{5+}_2O_6$	manganotapiolite	$Mn^{2+}_2Nb^{5+}_4O_{12}$
$Fe^{2+}_1Ta^{5+}_2O_6$	ferrotapiolite	$Fe^{2+}_2Ta^{5+}_4O_{12}$
$Mn^{2+}_1Ta^{5+}_2O_6$	manganotapiolite	$Mn^{2+}_2Ta^{5+}_4O_{12}$
Triple cation (disordered ? di- or tri-valent Fe ?)		
$(Ti,Nb,Fe)_1O_2$	ilmenorutile	$(Ti,Nb,Fe)_6O_{12}$
$(Ti,Ta,Fe)_1O_2$	strüverite	$(Ti,Ta,Fe)_6O_{12}$

The divalent transition element cation Ni^{2+} was recorded by Smith and Pinet (1985) but apparently no one has ever detected Co^{2+}. The large alkaline earth divalent cations Sr^{2+} and Ba^{2+}, as minor or trace constituents, are added by this work (see below). W^{6+} was recorded along with Sb^{5+} in rutile by Graham and Morris (1973). Zr^{4+} was added as a substituent in the review of oxides in lunar rocks by El Goresy (1976*a*); significantly, he did not mention Ti^{3+} in rutile although this reduced cation was mentioned in the armalcolite-'anosovite' (Ti_3O_5) series which coexists with rutile. Haggerty (1991) also recorded Zr^{4+}.

All the known single, double or triple cation mineral species with the disordered rutile structure are listed in Table 2 where it can be seen that the former are numerous and involve Ge^{4+}, Mn^{4+}, Pb^{4+}, Si^{4+}, Sn^{4+} and Te^{4+} (formulae and names from standard reference texts such as Fleischer and Mandarino, 1995, or from papers cited in this text for newer minerals). In contrast, only one double cation species is known in nature: squawcreekite, as mentioned above (Foord *et al.*, 1991) and related to rutile by mechanism (2) which is the one of principal interest here. The Ta^{5+} equivalent has been synthesized (Turnock, 1965). In these last two cited papers the double cation minerals were said to be disordered; it would however seem likely from charge-balance considerations that there exists at least some local ordering to reduce over- or under-charging the bridging oxygens of the shared octahedral edges.

The pentavalent cations Nb^{5+} and/or Ta^{5+} may provide valuable information on the behaviour of Sb^{5+}. Nb-rich rutile has been called 'ilmenorutile' and Ta-rich rutile 'strüverite' (e.g. Deer *et al.*, 1992), although the replacement of Ti does not seem to exceed 50 cat. % such that separate species names may not be merited. Fe is apparently always present in both 'species' as a lower-valent cation, otherwise some cation vacancies are necessary to accommodate the overcharged (Ti^{4+},Nb^{5+},Ta^{5+}) cation population. These are considered as triple cation disordered rutiles (Table 2) with the probable substitution:

$$2\ ^{vi}Ti^{4+} = {}^{vi}Fe^{3+} + {}^{vi}Nb/Ta^{5+} \qquad (3)$$

based on the cation exchange mechanism (1). If any Fe^{2+} is present then mechanism (5) (see below) may be invoked in addition.

The 'trirutile' structure of the tripuhyite/tapiolite mineral group is relevant here, even if the structure

is no longer strictly that of rutile since the cations are ordered. This involves the presence of relatively-large divalent cations regularly sandwiched between pentavalent cations along the octahedral chains, the *c* axis of which becomes tripled (e.g. Fig. 1 in Schmidbauer and Lebküchner-Neugebauer, 1987; Waychunas, 1991). Clark and Fejer (1978) presented X-ray data on twenty different natural tapiolites and deduced that several were in fact disordered. The question of ordering is not pursued here since the sole purpose of mentioning trirutiles is to demonstrate that, in addition to the pentavalent cations Sb^{5+}, Nb^{5+} and Ta^{5+} mentioned above, several divalent cations (Mg^{2+}, Mn^{2+}, Fe^{2+}, Zn^{2+}) can also enter the octahedral chains in substantial quantities; they do so in the proportion 1:2 $R^{2+} : R^{5+}$, in contrast to 1:1 $R^{3+} : R^{5+}$ in squawcreekite. Although the formula of the tripuhyite/tapiolite mineral group is given as $R^{2+}R^{5+}_2O_6$, Mn, Fe, Sb, Nb and Ta can all show several valency states so that it is not impossible that a mineral with an appropriate chemical composition could have a formula with another distribution of valencies such as $R^{3+}R^{4+}R^{5+}O_6$. The cation exchange mechanism which relates rutile to trirutile is:

$$3\ {}^{vi}R^{4+} = {}^{vi}R^{2+} + 2\ {}^{vi}R^{5+} \quad (4)$$

e.g.

$$3\ {}^{vi}Ti^{4+} = {}^{vi}Fe^{2+} + 2\ {}^{vi}Sb^{5+} \quad (5)$$

for tripuhyite.

Table 3 (after Shannon, 1976; updated by Bloss, 1994; reformulated by Perseil and Smith, 1995; and

TABLE 3. Ionic radii of the mentioned cations in six-fold co-ordination in the octahedral site of the tetragonal $P4_2/mnm$ rutile structure ${}^{vi}R^{4+}\ {}^{iii}O_2^{2-}$

Cation	Radius (Å)		Cation	Radius (Å)	
Si^{4+}	0.40		*Ti*$^{3+}$	*0.67*	
Cr^{5+}	*>.49*		Mn^{2+}	0.67	LS
Ge^{4+}	0.53		Nb^{4+}	0.68	
Mn^{4+}	0.53		Ta^{4+}	0.68	
Al^{3+}	0.54		Sn^{4+}	0.69	
V^{5+}	0.54		Ni^{2+}	0.69	
Cr^{4+}	*0.55*		Mg^{2+}	0.72	
Fe^{3+}	0.55	LS	Nb^{3+}	0.72	
Ni^{3+}	0.56	LS	Ta^{3+}	0.72	
Mn^{3+}	0.58	LS	Zr^{4+}	0.72	
V^{4+}	0.58		*Cr*$^{2+}$	*0.73*	*LS*
Sb^{5+}	0.60		Zn^{2+}	0.74	
Ti^{4+}	0.60		Sb^{3+}	0.76	
W^{6+}	0.60		Pb^{4+}	0.77	
Ni^{3+}	0.60	HS	Fe^{2+}	0.78	HS
Fe^{2+}	0.61	LS	V^{2+}	0.79	
Cr^{3+}	0.62		*Cr*$^{2+}$	*0.80*	*HS*
V^{3+}	0.64		Mn^{2+}	0.83	HS
Nb^{5+}	0.64		Te^{4+}	0.97	
Ta^{5+}	0.64		Ca^{2+}	1.00	
Fe^{3+}	0.64	HS	Sr^{2+}	1.18	
Mn^{3+}	0.64	HS	Ba^{2+}	1.35	

Chemical elements from the publications cited in the text.
Ionic radii from Bloss (1994).
LS = low spin; HS = high spin.
Double underlined = considered realistic in these samples.
Single underlined = considered doubtful in these samples.
Not underlined = not detected in these samples.
Italics = considered *unrealistic* in these samples.

augmented here) lists the effective ionic radii (in Å) in octahedral co-ordination of all of the mentioned cations, but with the addition of some other possible valencies for the same elements. It can thus be seen that trivalent Al, V, Cr, Mn, Fe and Ni, and pentavalent Sb, Nb and Ta, all have an ionic radius (0.54–0.64) close to that of tetravalent Ti (0.60). Furthermore, different valencies of these same elements are also considered possible from a purely crystal-chemical viewpoint (e.g. Mn^{4+} (0.53), V^{5+}, Nb^{4+}, Ni^{2+} (0.69) etc.). In contrast, we dismiss as unrealistic the highly oxidized cations Cr^{5+} and Cr^{4+} and the highly reduced ones Cr^{2+} and Ti^{3+}.

On the smaller ionic radius side, Si^{4+} (0.40) is considered too small to be able to share a disordered site with Ti^{4+}, although it does exist in pure stishovite (Table 2). Indeed octahedral Si is a typical feature only of ultra-high pressure or shock metamorphism (e.g. majorite, stishovite). All the reviews by Rumble (1976), Frost (1991) and Deer *et al.* (1992) mentioned the presence of Si without criticism. We consider that Si substitution in rutile is highly contentious at non-ultra-high pressure, and analysed Si is more likely to be due to analytical error, invisible microinclusions, or cations introduced into defective parts of the crystal structure.

On the larger ionic radius side, the recorded divalent Mg, V, Mn, Fe and Zn (high spin state) and tetravalent Sn, Zr, Pb and Te extend the size range from 0.69 to 0.97 which notably includes trivalent Sb (0.76). If ±0.20 Å (i.e. Si^{4+}) is considered too much of a difference in ionic radius to allow solid-solution with Ti^{4+}, then Sb^{3+} lies around the credibility limit for solid-solution in rutile. The high spin state for R^{2+} and R^{3+} was recommended by Shannon (1976), but not by Graham and Morris (1973) who worked with the low spin states, which makes an enormous difference (Table 3).

Apart from small Ge^{4+}, the remaining cations in Table 3 are the divalent alkaline-earths Ca, Sr and Ba, all of which would seem to be much too large; indeed they are the largest cations ever recorded in the rutile structure. They cannot however be rejected for the following reasons. If Ca could be regarded, like Si, as a simple analytical contaminant derived from the host grain, this cannot be the case of Sr since Ca≫Sr in the titanite host grain whereas Sr≫Ca in the rutile inclusions (Table 1). Since all of the divalent alkaline earth cations are only recorded as trace substituents, it is possible, again as suggested above for Si^{4+}, that they only occur in defective parts of the crystal-structure, or that they derive from invisible microinclusions of a Sr-rich phase such as strontianite; the relative constancy of the Sr concentrations and total absence of any supporting data render these hypotheses highly unlikely.

In terms of charge balance, the lower charge of divalent cations can easily be accommodated by the 'trirutile exchange mechanism' (4), i.e. for Sr:

$$3\ {}^{vi}Ti^{4+} = {}^{vi}Sr^{2+} + 2\ {}^{vi}Sb^{5+} \qquad (6)$$

by which a cation-charge-deficient $[Sr^{2+}O_6]^{10-}$ octahedron would be sandwiched inbetween two cation-charge-excess octahedra $[Sb^{5+}O_6]^{7-}$.

Alternatively the negative charge could be reduced by adding some protons, i.e.

$${}^{vi}Ti^{4+} + 2\ O^{2-} = {}^{vi}R^{2+} + 2\ (OH)^{-} \qquad (7)$$

In this case a few octahedra would be composed of $[SrO_4(OH)_2]^{8-}$ instead of $[TiO_6]^{8-}$. Minor substitution of O^{2-} by $(OH)^{-}$ in Al-, Cr-, Fe- and Nb-bearing rutile from eclogite has been deduced by infrared spectroscopy (Rossman and Smyth, 1990). Thus one can seriously envisage an exchange mechanism (7) in rutile similar to that now well-known in titanite:

$${}^{vi}Ti^{4+} + O^{2-} = {}^{vi}R^{3+} + (OH)^{-} \qquad (8)$$

(e.g. Smith, 1988; Oberti *et al.*, 1991; Perseil and Smith, 1995). However a preliminary microinfrared spectroscopic study of all of the Sb-rich rutile crystals described here did not reveal any OH bands.

As was the case with the host Sb-rich titanite grains (Perseil and Smith, 1995), several other elements should be able to accommodate themselves satisfactorily in the octahedral site within the rutile structure, e.g. As^{3+} (0.58), Mo^{5+} (0.61), Hf^{4+} (0.71), Cu^{2+} (0.73), U^{6+} (0.73), etc. (in Å). Cation vacancies may also occur; this point is discussed below along with the intriguing question of possible cation overpopulations.

Charge balance in Sb-rich rutile from St. Marcel-Praborna

The EMP analyses from the two petrographical environments in Table 1 are presented with the following valencies provisionally selected as 3^+ for Cr, Mn and Fe, and 5^+ for Sb on the bases of: 1. the ionic radii of the different possible valencies (Table 3), and 2. the deductions of the valency states of these cations in the host titanite grains of environment III (Perseil and Smith, 1995). The total wt.% values range between 98.79 and 100.64 %, except for one at 98.03 % which is less reasonable.

In these Sb-rich rutiles the relative importance of the trivalent cations is Fe ≫ Mn > Cr ~ Al (Table 1), whereas in the Sb-rich titanites of petrographical environments II and III the situation is more variable with the predominant relation being Al ~ Fe ≫ Mn > Cr (Perseil and Smith, 1995). Since only Al changes its relative position, one may deduce that the smaller cation Al can enter the rutile structure less

easily than the titanite structure (corner-sharing octahedral chain). In both environments II and III, up to around 40 cation % Ti in rutile may be replaced by the other cations, notably by up to 20 cation % Sb (Table 1); sample 9 is the Sb-richest rutile known to date at any locality, using the 50:50 terminological rule to separate rutile from squawcreekite. The natural samples of squawcreekite indicate between 58 and 71 % replacement of R^{4+} by $[R^{3+}_{0.5}R^{5+}_{0.5}]$ with considerable Sn^{4+} also replacing Ti^{4+} (Foord *et al.*, 1991).

For presenting the structural formulae, constant charges are problematical given the uncertain valencies of several cations and the uncertain presence of minor $(OH)^-$. Constant cations are preferred here (cf. for titanite in Perseil and Smith, 1995). On the basis of sum cations = 1.000, the sum oxygens value ranges between 1.988 and 1.999 for 8 out of 9 analyses. The corresponding charge excess thus varies from −0.024 (0.6 relative % of 4.000 charges) to −0.002. These values, which thus correspond to anion 'underpopulations' (or to cation 'overpopulations' if recalculated on the basis of sum oxygens = 2.000), are frequently small enough to be accounted for by general analytical precision and accuracy (e.g. maximum one sigma = +0.003 in cations or +0.015 in charges for Sb, Table 1).

These negative cumulated charge excesses (or cumulated charge deficiencies) could however be alternatively accounted for by a cation having been attributed a valency too low; the only possibility is Mn since Cr is hardly present: converting some or all Mn^{3+} into Mn^{4+} would eliminate the charge imbalance in all but one sample. It is well-known that Mn may possess more than one valency in the same mineral species (e.g. both Mn^{3+} and Mn^{4+} in romanéchite and todorokite). This does not mean that some or all Mn has to be tetravalent, but it does show that all the cations do have to be in a rather high oxidized state such that the presence of low-valent Mn^{2+}, Fe^{2+}, and especially Sb^{3+} and Ti^{3+}, are not invoked here, in contrast to the situation in the host Sb-rich titanites where positive cumulated charge excesses are common (Perseil and Smith, 1995). A further hypothesis is that some $(OH)^-$ is actually present; introducing protons has the unique advantage of increasing the overall positive charge (or decreasing the overall negative charge, depending upon whether one prefers to consider H^+ or $(OH)^-$ respectively) without increasing the population of the octahedral site.

The only R^{4+} cation detected, other than obvious Ti^{4+}, improbable Si^{4+} and debatable Mn^{4+}, is Zr^{4+} which occurs sporadically in negligible proportions. Cation exchange between these tetravalent cations of course has no effect on the charge balance. If no monovalent, divalent or hexavalent cations were present, then in terms of cation quantities the important relation:

$$\Sigma\ ^{vi}R^{5+} = \Sigma\ ^{vi}R^{3+} \qquad (9)$$

must hold, according to mechanisms (1) and (2). Table 1 shows that the values of $[\Sigma R^{5+} - \Sigma R^{3+}]$ vary between −0.015 and +0.018 but are more often negative, i.e. excess R^{3+}.

In terms of cation charges, the differences $[\Sigma R^{5+} - \Sigma R^{3+}]$ have the same values since the valencies of both of the incoming cations differ from that of the outgoing cation by just one charge. A value of zero would correspond to the perfect exchange mechanism (1), as expanded into precise cations in mechanism (2). The general excess of R^{3+} again indicates no need nor possibility of converting some Sb^{5+} into Sb^{3+}, or $(Mn,Fe)^{3+}$ into $(Mn,Fe)^{2+}$. The same argument also indicates that no Sb^{4+} is present by way of the hypothetical simple homovalent mechanism:

$$^{vi}Ti^{4+} = {}^{vi}Sb^{4+} \qquad (10)$$

Sb^{4+} seems to be generally ignored in the geological literature although Pascal (1958, p. 527) and Heslop and Robinson (1963, p. 344) emphasized the strong covalent nature of much of the bonding of this semi-metal such that any purely ionic notation is imprecise. In terms of ionic notation Sb^{4+} is indicated in the solid state in antimony tetroxide Sb_2O_4 (Pascal, 1958), unless it is a mixture of Sb^{3+} + Sb^{5+} as presented in cervantite $Sb^{3+}Sb^{5+}O_4$ (Fleischer and Mandarino, 1995).

The small amounts of divalent cations present, especially Sr^{2+}, must be taken into account and they would be expected to improve the charge balance. They are nevertheless so small that the range of the new algebraic sum of charges $[\Sigma R^{5+} - \Sigma R^{3+} - 2\ \Sigma R^{2+}]$ (Table 1) is similar (−0.024 to +0.011) compared to ignoring R^{2+}. Indeed these new values are identical to the 'charge excess' values cited above since, in terms of cation charges, the perfect equivalence:

$$^{vi}R^{5+} = {}^{vi}R^{3+} + 2\ {}^{vi}R^{2+} \qquad (11)$$

(i.e. the charge excess compared to Ti^{4+} on the left should equal the cumulated charge deficiency on the right) would leave as a residue exactly the analytical uncertainty values manifested in the 'charge excess' (N.B. in Table 1 there is no R^{6+} nor OH^- to perturb this relationship). All but one of these sums corrected for R^{2+} are negative such that the situation is not improved compared to ignoring R^{2+}. Thus, on the basis of charge balance, one could largely set aside the role of the divalent cations, especially the sporadic and low values for Ca^{2+} and Ba^{2+}. However it should be noted that at St. Marcel-Praborna, Sr and sometimes also Ba appear at a late-stage in many mineral phases: Sr-rich piemontite (Perseil, 1987); titanite (Perseil and

Smith, 1995); Mn-oxides (intermediate members of the cryptomelane–hollandite series) (Perseil, 1988); and now strontiomelane (Perseil *et al.*, in prep.) [a new mineral species accepted by the IMA in 1995: the Sr-equivalent of the cryptomelane (K) – hollandite (Ba) series showing that there is extensive solid-solution between the Sr, K and Ba end-members]. Thus a minor incorporation of these pervasive alkaline earth elements into rutile at the same locality would not be surprising.

Statistical correlations

Having treated the data in tabular form, they can now be evaluated in graphic form in order to examine any

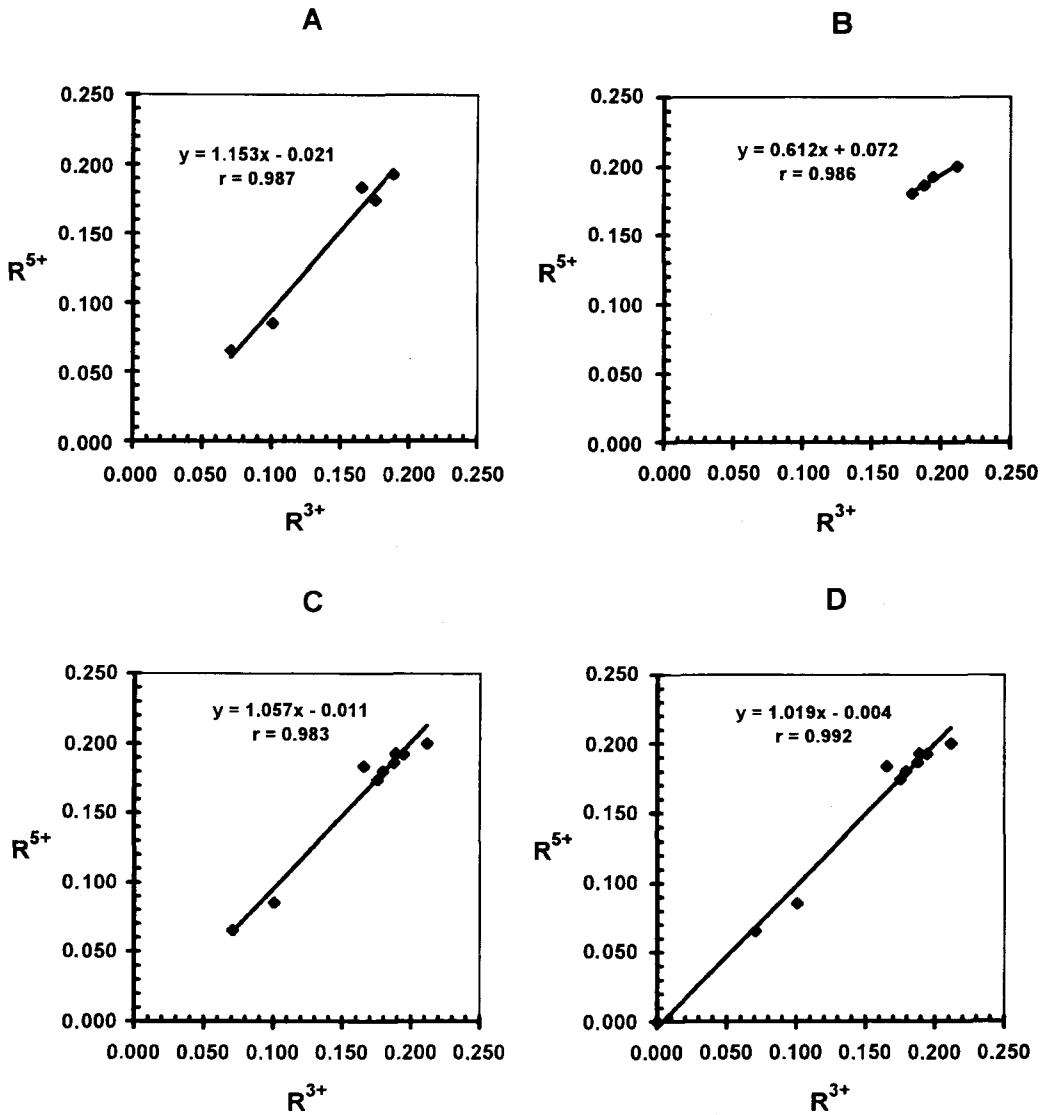

FIG. 7. Chemical plots of R^{5+} against $R^{3+} = [Al^{3+} + Cr^{3+} + Mn^{3+} + Fe^{3+}]$ for Sb-rich rutile from environment II (A); from environment III (B); from both environments superimposed (C); and both environments with an artificial data point added at the origin (see text) (D).

trends that may be present. The data values are taken from Table 1 without any changes in valencies. ΣR^{5+} is plotted against ΣR^{3+} in Figs. 7A–D in order to test relation (9).

The data points from petrographical environment III tend to cluster together and hence do not reveal a strong and significant trend (r = 0.986, n = 4, Fig. 7B). On the contrary, the two low values from petrographical environment II create a more convincing strong trend (r = 0.987, n = 5, Fig. 7A) tending towards the origin with a slope close to 1 (+1.153) and an ordinate intercept close to zero (−0.021).

In Fig. 7C, both data sets are superimposed and it can be seen that they belong to comparable populations (in chemical terms but not in petrographical terms) such that the superposition is statistically valid. Thus there is no significant difference between the crystal-chemistry of the Sb-rich rutiles from the two different petrographical environments. Furthermore, although the correlation coefficient is slightly lower (r = 0.983, n = 9), n is larger and hence r is in fact statistically more significant. Also the slope is closer to 1 (+1.057) and the ordinate intercept is closer to 0 (−0.011) compared to Fig. 7A.

Substitution (2) with its definitive relation (9) is thus identified here as the major cation exchange mechanism in these samples of Sb-rich rutile. This can be simply modelled by merely constraining the trend to pass close to the origin by adding an artificial data point at $\Sigma R^{5+} = \Sigma R^{3+} = 0.000$ which represents the starting point of this trend in pure rutile. The result in Fig. 7D reveals an increased r value (0.992, n = 10) with even greater statistical significance from which it is deduced that the data and the model are perfectly compatible within the limits of analytical uncertainty. As in the case of Sb-rich titanite, Moore's (1968) early prediction of the importance of the $[(Mn+Fe)^{3+} + Sb^{5+}]$ mechanism for the replacement of Ti^{4+} in Ti-Mn-Fe oxides and silicates is confirmed; however Al^{3+} and Cr^{3+} should be added to R^{3+}.

It may be noted that in Figs. 7A, 7C and 7D the slope slightly exceeds 1 but with a negative ordinate at $x = 0$. This represents the slight relative excess of R^{3+}, or deficiency of R^{5+}, at $x = 0$ which is largely maintained at high x values (Table 1). This relative excess of R^{3+} is compatible with the real presence of minor Mn^{4+} and hence with less Mn^{3+}. It is also compatible with the real presence of minor $(OH)^-$ which would 'consume' some R^{3+} by mechanism (8). Any $(OH)^-$ concerned by mechanism (7) would not be visible in the plots of Fig. 7. It is particularly important to notice that it cannot be explained by the involvement of mechanism (6) which 'consumes' some R^{5+} and would thus aggravate the R^{3+} charge excess; hence this provides evidence against the action of the trirutile mechanisms (4), (5) and (6) in these samples, i.e. it opposes the presence of both (Mn^{2+},Fe^{2+}) and of the alkaline earths in the octahedral chains.

Crystallographical positioning of the large divalent cations: chain undercharge and tunnel occupation?

As in many mineral groups, cation or even anion vacancies in rutile are not impossible. Single heterovalent substitutions like the hypothetical solution of Fe_2O_3 (= $Fe_1O_{1.5}{}^*{}_{0.5}$ = $Fe_{\underline{1.33}}O_2$) or of Nb_2O_5 (= $Nb_1O_{\underline{2.5}}$ = $Nb_{0.8}{}^*{}_{0.2}O_2$) [where * = vacancy or underpopulation, and underlining = overpopulation] must lead to anion or cation vacancies or overpopulations as indicated in the brackets. It was assumed above that Fe^{3+} in rutile occurs in the octahedral site along with the other trivalent cations, Ti^{4+} and Sb^{5+}. However it has been suggested (Waychunas, 1991, p. 40) that at high T Fe^{3+} may enter other sites, normally unoccupied, in rutile, in particular a set of sites analogous to those in hematite. These sites are precisely those within the tunnels. Also Waychunas (1991, p. 18) mentioned that these tunnels 'allow considerable diffusion' without specifying what size of cations. Given the cation overpopulation with dissolved hematite, it is almost inescapable that a quarter of the Fe^{3+} cations lie in the tunnel sites (one could argue for oxygen vacancies). Overcharge in the adjacent octahedra in the chains could be accommodated by placing the other Fe^{3+} cations there rather than Ti^{4+}, i.e. by the general cation exchange mechanism:

$$3\ {}^{vi}R^{4+} + {}^{tunnel}\text{vacant} = 3\ {}^{vi}R^{3+} + {}^{tunnel}R^{3+} \quad (12)$$

which here becomes:

$$3\ {}^{vi}Ti^{4+} + {}^{tunnel}\text{vacant} = 3\ {}^{vi}Fe^{3+} + {}^{tunnel}Fe^{3+} \quad (13)$$

Overcharge could also be accommodated by a few vacancies in the octahedral chains; this is in fact the situation in the pure hematite structure which is essentially equivalent to that of a rutile structure having one third of all the chain sites and one third of all the tunnel sites vacant (compare Figs. 6c and 9c in Waychunas, 1991), i.e.

$$\begin{aligned} 3\ {}^{vi}Ti^{4+} + 3\ {}^{tunnel}\text{vacant} \quad & [\text{RUTILE}] \\ = 2\ {}^{vi}Fe^{3+} + 2\ {}^{tunnel}Fe^{3+} + 1\ {}^{vi}\text{vacant} + & \\ 1\ {}^{tunnel}\text{vacant} \quad & [\text{HEMATITE}] \end{aligned} \quad (14)$$

This possibility opens up a whole new dimension to the problem by allowing incomplete occupation of the octahedral chains with the total sum of cations exceeding 1 per O = 2. At St. Marcel-Praborna, Fe^{3+} or the other trivalent cations do not pose a problem as several of the mechanisms listed above can explain their presence within the octahedral chains or the

tunnels. The interesting question here is the divalent cations from the point of view of charge and of ionic radius.

The chemical analyses of Table 1 are not all recalculated again according to these hypotheses since (1) it is no longer known to what value the sum of the cations should be recalculated, and also (2) because it would involve small calculations mostly within the limits of the analytical uncertainties. It may suffice to record that excluding the alkaline earths and then fixing Σ cations = 1, i.e. octahedral chains = full and all alkaline earths situated in the tunnels, would increase all the cation and anion values such that the oxygen deficiency would disappear along with the hypotheses of the presence of OH^- or Mn^{4+}.

That the alkaline earth cations seem to be much too large for the octahedral sites of rutile (Table 3) is not a new problem in mineralogy (cf. the long-standing debate over K^+ being too large to enter the pyroxene structure). In a perfectly-regular (oxygen planes perfectly flat) rutile-like structure, the interstices within the tunnels would have exactly the same shape and size as the octahedral sites within the chains, but the real rutile structure is slightly distorted. In an octahedral interstice within a tunnel there are other oxygens not very far away. It is thus quite conceivable that a distorted site with co-ordination > 6 (8–12, like 12-fold K^+ but 6-fold Na^+ in micas since for larger K^+ the 'outer' oxygens are counted as well as the 'inner' ones) could be obtained which would be appropriate for occupancy by Ca^{2+}, Sr^{2+} or Ba^{2+}. This new site would not be expected to have the same *c* co-ordinate as the octahedral cations, but this is precisely the situation of the large alkaline earth or alkali cations which occupy the wider tunnels provided in the rather similar structures of the cryptomelane/hollandite/priderite group (2 × 2), romanéchite (2 × 3) and todorokite (3 × 3) where the numbers refer to the number of octahedra counted along the edges of the tunnel (1 × 1 for rutile) (compare Figs. 6a, 12b, 21 and 22 in Waychunas, 1991). OH^- or H_2O is also recorded in these minerals.

Indirect support for tunnel occupancy in the rutile structure comes from the data of Perseil and Grandin (1978) on the gradual natural transformation of pyrolusite (Table 2) into cryptomelane. This involves the incorporation of the large K^+ cation into tunnel sites, the reduction of the average valency of Mn, and a short migration of many Mn cations in order to create (2 × 2) tunnels. Although, strictly-speaking, once this overall process had begun the structure was no longer that of pyrolusite, the process had to begin somewhere and this could well have been achieved by a K^+ cation trying to enter a peripheral tunnel site. In the Sr-bearing Sb-rich rutiles from St. Marcel-Praborna it is not impossible that the minor Sr presence likewise represents a transitional stage in the local transformation of rutile into an Sb-Sr-equivalent of priderite $(K,Ba)(Ti,Fe^{3+})_8O_{16}$ or an Sb-Ti-Fe-equivalent of strontiomelane $(Sr)(Mn^{4+},Mn^{2+})_8O_{16}$. It so happens that both Sr-bearing priderite (Perseil, 1991) and strontiomelane (Perseil *et al.*, in prep.) occur in the manganese concentrations at St. Marcel-Praborna.

It is thus concluded that there is a strong possibility that the divalent alkaline earth cations enter the tunnels in the rutile structure rather than the octahedral chains. This is best represented by the new cation exchange mechanism:

$$2\ {}^{vi}R^{4+} + {}^{tunnel}\text{vacant} = 2\ {}^{vi}R^{3+} + {}^{tunnel}R^{2+} \quad (15)$$

This mechanism conveniently 'consumes' some R^{3+} without involving any R^{5+}. It thus provides an excellent explanation of the minor relative excess of ΣR^{3+} over ΣR^{5+} described above (Fig. 7).

The entry of a few large divalent cations into tunnel sites raises a tantalising question: can this local redistribution of charge and of geometric parameters modify the local thermodynamic situation such that a particular site becomes small enough to allow a small Si^{4+} cation to slip in? But if so, is it still reasonable to employ the term 'rutile' for a local Si+[Sr+Ba] cation association? The fact that our unpublished full raw data set reveals a positive correlation between the presences of traces of Si and of Ba requires that such a cation association should not be hastily ruled out.

Conclusions

1. The two hypotheses of Sb-metasomatism of pre-existing rutile (c) and of the growth of neoblastic Sb-rich rutile (d) at St. Marcel-Praborna (Perseil and Smith, 1995) are both considered confirmed by the new data; it is suggested that Fig. 4 demonstrates the operation of both processes in a single rutile grain.

2. The highest Sb concentrations (0.2 Sb per O = 2) at St. Marcel-Praborna are the highest recorded anywhere in rutile and approach the 50:50 terminological limit ($Fe^{3+}_{0.25}Sb^{5+}_{0.25}Ti^{4+}_{0.50}O_2$) towards the ideal end-member mineral squawcreekite $FeSbO_4$.

3. A crystal-chemical evaluation establishes that the predominant, almost exclusive, cation exchange mechanism is:

$$2\ {}^{vi}R^{4+} = {}^{vi}R^{3+} + {}^{vi}R^{5+} \quad (1)$$

within the octahedral chain; this is perturbed only by a minor excess of R^{3+} and a minor charge deficit on the basis of Σ cations = 1. This is also the predominant mechanism in the Sb-rich titanite.

4. Small amounts of large divalent alkaline earth elements are present and could be explained by a

local expression of the 'trirutile' mechanism:

$$3\ {}^{vi}R^{4+} = {}^{vi}R^{2+} + 2\ {}^{vi}R^{5+} \quad (4)$$

However several other hypotheses are discussed because these are the largest cations ever recorded in the rutile structure and they may not be able to enter the normal octahedral sites. The favoured interpretation is provocative but defendable: that Ca, Sr and Ba are located within the lozenge-shaped tunnels of the rutile structure according to the new cation exchange mechanism:

$$2\ {}^{vi}R^{4+} + {}^{tunnel}\text{vacant} = 2\ {}^{vi}R^{3+} + {}^{tunnel}R^{2+} \quad (15)$$

analogous to the situation in many other oxides which have larger tunnels. This mechanism is also supported by the fact that it largely resolves the minor problem of R^{3+} exceeding R^{5+} in these samples.

5. The probabilities of the presence in rutile at St. Marcel-Praborna of a particular ion in terms of its charge and size, and the site co-ordination, are evaluated as follows:

unrealistic: ${}^{vi}Cr^{5+}$, ${}^{vi}Cr^{4+}$, ${}^{vi}Cr^{2+}$ and ${}^{vi}Ti^{3+}$;
improbable: ${}^{vi}Si^{4+}$, ${}^{vi}Sb^{4+}$, ${}^{vi}Sb^{3+}$, ${}^{vi}(Mn,Fe)^{2+}$, and ${}^{vi}(Ca,Sr,Ba)^{2+}$;
possible: ${}^{vi}Mn^{4+}$ and OH^{-};
probable: ${}^{tunnel}(Ca,Sr,Ba)^{2+}$;
realistic: ${}^{vi}Sb^{5+}$, ${}^{vi}(Ti,Zr)^{4+}$ and ${}^{vi}(Al,Cr,Mn,Fe)^{3+}$.

Acknowledgements

We are grateful to M. Marot for carefully preparing the thin sections and to P.Blanc for efficiently helping with the SEM technique. An unnamed reviewer suggested useful improvements to the text.

References

Bloss, F.D. (1994) *Crystallography and Crystal-chemistry*. Mineral. Soc. Amer., Washington, 545 pp.

Clark, A.M. and Fejer, E.E. (1978) Tapiolite, its chemistry and cell dimensions. *Mineral. Mag.*, **42**, 477–80.

Deer, W.A., Howie, R.A. and Zussman, J. (1992) *An Introduction to the Rock-Forming Minerals*. Longman Scientific and Technical, Harlow, Essex, U.K., 696 pp.

El Goresy, A. (1976*a*) Oxide minerals in lunar rocks. Chap. 5, p. EG1–EG46. In *Reviews in Mineralogy*, Mineral. Soc. Amer., **3**, Oxide Minerals, (ed.) D. Rumble III.

El Goresy, A. (1976*b*) Oxide minerals in meteorites. Chap. 6, p. EG47–EG72. In *Reviews in Mineralogy*, Mineral. Soc. Amer., **3**, Oxide Minerals, (ed.) D. Rumble III.

Fleischer, M. and Mandarino, J.A., (1995) Glossary of mineral species 1995. *The Mineral Record*, Tucson, Arizona 280 pp.

Foord, E.E., Hlava, P.F., Fitzpatrick, J.J., Erd, R.C. and Hinton, R.W. (1991) Maxwellite and squawcreekite, two new minerals from the Black Range tin district, Catron County, New Mexico, U.S.A.. *Neues Jahrb. Mineral. Monat.*, 363–84.

Frost, B.R. (1991) Stability of oxide minerals in metamorphic rocks. Chap. 13, p. 469–487. In *Reviews in Mineralogy*, Mineral. Soc. Amer., **25**, Oxide Minerals: petrologic and magnetic significance, (ed.) D.H. Lindsley.

Graham, J. and Morris, R.C. (1973) Tungsten- and antimony-substituted rutile. *Mineral. Mag.*, **39**, 470–3.

Haggerty, S.E. (1991) Oxide mineralogy of the upper mantle. Chap. 10, p. 355–416. In *Reviews in Mineralogy*, Mineral. Soc. Amer., **25**, Oxide Minerals: petrologic and magnetic significance, (ed.) D.H. Lindsley.

Heslop, R.B. and Robinson, P.L. (1963) *Inorganic Chemistry: a Guide to Advanced Study*. Elsevier, Amsterdam, 591 pp.

Lasnier, B., Poirot, J.-P. and Smith, D.C. (1992) Intercroissances de jadéite de différentes compositions dans des jades révélées par cathodoluminescence. *Revue de Gemmologie*, A.F.G., Paris, **113**, 8–11.

Lindsley, D.H. (1991) Experimental studies of oxide minerals. Chap. 3, p. 69–106. In *Reviews in Mineralogy*, Mineral. Soc. Amer., **25**, Oxide Minerals: petrologic and magnetic significance, (ed.) D.H. Lindsley.

Martin, S. and Kienast, J.-R. (1987) The HP-LT manganiferous quartzites of Praborna, Piemonte ophiolite nappe, Italian Western Alps. *Schweiz. Mineral. Petrogr. Mitt.*, **67**, 339–60.

Moore, P.B. (1968) Substitutions of the type $(Sb^{5+}_{0.5}Fe^{3+}_{0.5}) = (Ti^{4+})$: the crystal structure of melanostibite. *Amer. Mineral.*, **53**, 1104–9.

Morgan, B.A. (1975) Mineralogy and origin of skarns in the Mount Morrison Pendant, Sierra Nevada, California. *Amer. J. Sci.*, **275**, 119–42.

Mottana, A. (1986) Blueschist-facies metamorphism of manganiferous cherts: A review of the alpine occurrences. *Geol. Soc. Amer. Memoir*, **164**, 267–99.

Oberti, R., Smith, D.C., Rossi, G. and Caucia, F. (1991) The crystal-chemistry of high-aluminium titanites. *European J. Mineral.*, **3**, 777–92.

Parent, C. and Roger, G. (1968) Le gîte antimonifère de Buzeins (Aveyron). Un exemple de minéralisation épigénétique 'familière' dans l'Autunien. Source de la minéralisation et rôle de la matière organique. *Bull. B.R.G.M., 2 e série, sect. II*, **4**, 1–41.

Pascal, P. (1958) *Nouveau Traité de Chimie Minérale: Tome XI: arsenic - antimoine - bismuth.* Masson, Paris.

Perseil, E.-A. (1985) Quelques caractéristiques des faciès à oxydes de manganèse dans le gisement de St. Marcel-Praborna (Val d'Aoste, Italie). *Mineral. Deposita*, **20**, 271–6.

Perseil, E.-A. (1987) Particularités des piémontites de Saint-Marcel-Praborna (Italie): Spectres I.R. *Actes du 112e Congrès National Sociétés Savantes, Lyon, Section Sciences*, **Fasc. I**, 209–15.

Perseil, E.-A. (1988) La présence du strontium dans les oxydes manganésifères du gisement de St. Marcel-Praborna (Val d'Aoste, Italie). *Mineral. Deposita*, **23**, 306–8.

Perseil, E.-A. (1991) La présence de Sb-rutile dans les concentrations manganésifères de St. Marcel-Praborna (Val d'Aoste, Italie). *Schweiz. Mineral. Petrog. Mitt.*, **71**, 341–7.

Perseil, E.-A. and Grandin, G. (1978) Evolution minéralogique du manganèse dans trois gisements d'Afrique de l'Ouest: Mokta, Tambao, Nsuta. *Mineral. Deposita*, **13**, 295–311.

Perseil, E.-A. and Smith, D.C. (1995) Sb-rich titanite in the manganese concentrations at St. Marcel-Praborna, Aosta Valley, Italy: petrography and crystal-chemistry. *Mineral. Mag.*, **59**, 717–34.

Perseil, E.-A. and Smith, D.C. (1996) Cristallochimie de l'arsenic dans la fluorapatite et la titanite des concentrations manganésifères de St. Marcel-Praborna, V. Aoste (Italie). *Réunion biennale française RST*, Orléans, Résumés, 167.

Perseil, E.-A., Blanc, P. and Smith, D.C. (1996) Modification of the luminescence of fluorapatite: replacement of phosphorus by arsenic in the fluorapatites of the manganese concentrations at St. Marcel, Aosta, Italy. *Internat. Conf. Cathodoluminescence*, Nancy, France, Abstracts, 111–2.

Pinet, M. and Smith, D.C. (1985) Petrochemistry of opaque minerals in eclogites from the Western Gneiss Region, Norway. 1. Petrology of the oxide microassemblages. *Chem. Geol.*, **50**, 225–49.

Putnis, A. (1978) The mechanism of exsolution of hematite from iron-bearing rutile. *Phys. Chem. Mineral.*, **3**, 183–97.

Roger, G. (1972) Un type de minéralisations épigénétiques familières: les filons à antimoine du Massif Central français. Hypothèse de la sécrétion latérale. *Mineral. Deposita*, **7**, 360–82.

Rossman, G.R. and Smyth, J. (1990) Hydroxyl contents of accessory minerals in mantle eclogites and related rocks. *Amer. Mineral.*, **75**, 775–80.

Rumble III, D. (1976) Oxide minerals in metamorphic rocks. Chap. 3, p. R1–R24. In *Reviews in Mineralogy*, Mineral. Soc. Amer., **3**, Oxide Minerals, (ed.) D. Rumble III.

Schmidbauer, E. and Lebküchner-Neugebauer, J. (1987) ^{57}Fe Mössbauer study on compositions of the series $Fe^{3+}TaO_4 - Fe^{2+}Ta_2O_6$. *Phys. Chem. Minerals*, **15**, 196–200.

Shannon, R.D. (1976) Revised effective ionic radii and systematic studies of interatomic distances in halides and chalcogenides. *Acta Crystallogr.*, **A32**, 751–67.

Smith, D.C. (1988) A review of the peculiar mineralogy of the 'Norwegian Coesite-Eclogite Province', with crystal-chemical, petrological, geochemical and geodynamical notes and an extensive bibliography. In *Eclogites and Eclogite-Facies Rocks*, (D.C. Smith, ed.), *Developments in Petrology*, **12**, 1–206. Elsevier, Amsterdam, 524 pp.

Smith, D.C. and Perseil, E.-A. (1996) Cristallochimie de l'antimoine dans la titanite, le rutile et la roméite des concentrations manganésifères de St. Marcel-Praborna, V. Aoste (Italie). *Réunion biennale française RST*, Orléans, Résumés, 168.

Smith, D.C. and Pinet, M. (1985) Petrochemistry of opaque minerals in eclogites from the Western Gneiss Region, Norway. 2. Chemistry of the ilmenite mineral group. *Chem. Geol.*, **50**, 251–66.

Turnock, A.C. (1965) Fe–Ta oxides: phase relations at 1200°C. *J. Amer. Ceram. Soc.*, **48**, 258–61.

Waychunas, G.A. (1991) Crystal-chemistry of oxides and oxyhydroxides. Chap. 2, p. 11–68. In *Reviews in Mineralogy*, Mineral. Soc. Amer., **25**, Oxide Minerals: petrologic and magnetic significance, (ed.) D.H. Lindsley.

Yardley, B., Rochelle, C.A., Barnicoat, A.C. and Lloyd, G.E. (1991) Oscillatory zoning in metamorphic minerals: an indicator of infiltration metasomatism. *Mineral. Mag.*, **55**, 357–65.

[*Manuscript received 11 September 1996: revised 23 January 1997*]